

Prediction of anomalies in the velocity of sound for the pseudogap of hole-doped cuprates

C. Walsh,¹ M. Charlebois,² P. Sémon,³ G. Sordi,^{1,*} and A.-M. S. Tremblay³

¹*Department of Physics, Royal Holloway, University of London, Egham, Surrey, UK, TW20 0EX*

²*Département de Chimie, Biochimie et Physique, Institut de Recherche sur l'Hydrogène, Université du Québec à Trois-Rivières, Trois-Rivières, Québec, Canada G9A 5H7*

³*Département de physique, Institut quantique & RQMP, Université de Sherbrooke, Sherbrooke, Québec, Canada J1K 2R1*

(Dated: December 21, 2022)

We predict sound anomalies at the doping δ_p where the pseudogap ends in the normal state of hole-doped cuprates. Our prediction is based on the two-dimensional compressible Hubbard model using cluster dynamical mean-field theory. We find sharp anomalies (dips) in the velocity of sound as a function of doping and interaction. These dips are a signature of supercritical phenomena, stemming from an electronic transition without symmetry breaking below the superconducting dome. If experimentally verified, these signatures may help to solve the fundamental question of the nature of the pseudogap – pinpointing its origin as due to Mott physics and resulting short-range correlations.

I. INTRODUCTION

Upon decreasing the temperature near half-filling, cuprate superconductors reach a temperature T^* where spin susceptibility and photoemission experiments show features that suggest a loss in the density of states. This has been associated to a so-called pseudogap phase, with T^* a crossover rather than a sharp phase transition^{1,4}. In addition, below T^* as defined above, broken symmetry states are observed by some probes^{1,3}. At even lower temperature, superconductivity and charge-density wave phases appear^{1,3}. On the other hand, in 2018, experiments revealed that thermodynamic properties show signatures of a phase transition upon crossing the critical doping δ_p where the pseudogap ends at low temperature, such as a sharp peak in the specific heat². Even more puzzling, this thermodynamic signature of a transition occurs without a detectable diverging correlation length associated to a broken symmetry state^{1,2}.

The two-dimensional (2D) Hubbard model in the doped Mott insulator regime⁴ captures these aforementioned key features that are consistent with the observed pseudogap – namely (i) that the pseudogap is a crossover across T^* and (ii) there is a phase transition across δ_p at low T , (iii) without the need of a broken symmetry state, (iv) which can however appear within the pseudogap phase. In particular, studies on this model based on cluster extensions of dynamical mean-field theory⁵ revealed that the phase transition across δ_p is a metal to metal first-order transition without symmetry breaking^{6,7}, due to Mott physics and short range correlations. This transition ends at finite doping and finite temperature in a second order critical point, from which supercritical crossovers emerge^{8,9}. This theoretical framework resolves the paradox of the thermodynamic anomalies at the endpoint of the pseudogap (e.g. the peak in the specific heat across δ_p) without the need for broken symmetry states, as discussed in Refs.^{10,11}.

In this article we provide a novel and crucial *prediction*

of this theoretical framework for ultrasound experiments in hole-doped cuprates. The propagation of sound is a powerful tool to characterise phase transitions in solids because it is a sensitive way of probing the thermodynamics of a system. We shall prove that the velocity of sound has signatures of a phase transition across δ_p and of a crossover across T^* . Crucially, if confirmed by experiments, this will provide further decisive evidence that the pseudogap arises from Mott physics and short-range correlations.

Recent advances in ultrasound techniques should enable the testing of our prediction. Indeed, the last few years have witnessed a renewed attention in using ultrasounds to probe electronic phase transitions in strongly correlated electron systems, and experimental findings motivate new theoretical investigations. For example, an experiment¹² in the cuprate $\text{YBa}_2\text{Cu}_3\text{O}_{6+x}$ (YBCO) found a break in the slope of the velocity of sound at the onset of the pseudogap, suggestive of a phase transition, although this interpretation has been challenged in Ref.¹³. In another cuprate, $\text{La}_{2-x}\text{Sr}_x\text{CuO}_4$ (LSCO), ultrasound anomalies were connected to the coupling between the lattice and the spin glass^{14,15}. In other correlated electron systems, ultrasounds were used to place constraints on the order parameter symmetry of the hidden order in URu_2Si_2 ¹⁶ and in the superconducting state of Sr_2RuO_4 ^{2,18}. Anomalies in the velocity of sound have been used to describe the crossover emerging from the Mott transition in V_2O_3 ¹⁹ and organic superconductors^{20,21}. Our contribution in this article is to identify how the velocity of sound captures the pseudogap emerging from Mott physics and resulting short-range correlations.

II. MODEL AND METHOD

The velocity of sound c_s along high symmetry directions is defined as $c_s = \sqrt{c_{ij}/\rho}$, where ρ is the density,

$c_{ij} = \partial^2 F / \partial u_{ij}^2$ is the elastic constant in the Voigt notation, F is the free energy, and u_{ij} is the strain, also in Voigt notation. Cuprates have tetragonal (D_{4h}) symmetry, and in this work we focus on the uniform compressive strain in the xy plane, which is associated to the elastic constant $c_{A_{1g}} = (c_{11} + c_{22})/2$ of the A_{1g} irreducible representation. Furthermore, we consider both electronic and lattice degrees of freedom. Hence the free energy is the sum of two terms: the electronic free energy F_{el} and the lattice free energy F_{latt} , with $F_{\text{el}} = F_0 + F_{\text{el-latt}}$, where F_0 is the free energy of the electrons at zero strain and $F_{\text{el-latt}}$ is the free energy due to the interaction between electrons and the lattice. The elastic constant of the A_{1g} mode, and hence its associated velocity of sound, is renormalised by the interaction between electrons and lattice as $c_{A_{1g}}^* = c_{A_{1g}} + \Delta c_{A_{1g}}$, where $\Delta c_{A_{1g}}$ is the correction to $c_{A_{1g}}$ due to the electron-lattice interaction, i.e. physically it is the contribution to the elastic stiffness due to the electrons at the Fermi level.

To find $\Delta c_{A_{1g}}$, we consider the following Su-Schrieffer-Heeger-Hubbard Hamiltonian³ on the 2D square lattice:

$$H = - \sum_{\langle ij \rangle \sigma} t [a + (d_i - d_j)] (c_{i\sigma}^\dagger c_{j\sigma} + c_{j\sigma}^\dagger c_{i\sigma}) + U \sum_i n_{i\uparrow} n_{i\downarrow} - \mu \sum_{i\sigma} n_{i\sigma}. \quad (1)$$

Eq. 1 can be viewed as a *compressible* Hubbard model, as in Refs.^{4,5}. Here $c_{i\sigma}^\dagger, c_{i\sigma}$ create and destroy, respectively, an electron at site i of spin σ , $n_i = c_{i\sigma}^\dagger c_{i\sigma}$ is the number operator, U is the onsite Coulomb interaction, and μ is the chemical potential. Contrary to the (standard) Hubbard model, the nearest neighbor hopping amplitude t is modulated by the local change ($d_i - d_j$) of the equilibrium lattice constant a , i.e. with zero wavevector as appropriate for ultrasound experiments. This Hamiltonian preserves electroneutrality.

For the 2D compressible Hubbard model with nearest-neighbor hopping in Eq. 1, the correction $\Delta c_{A_{1g}}$ to the elastic constant $c_{A_{1g}}$ due to the interaction between electrons and lattice is given by the second derivative of the electronic free energy with respect to hopping, $\partial^2 F_{\text{el}} / \partial t^2$, which is proportional to $\partial \langle \epsilon \rangle / \partial t$, where $t \langle \epsilon \rangle$ is the kinetic energy of the 2D Hubbard model (see derivation in the supplemental material²⁵). This in turn determines the velocity of sound of the A_{1g} mode. To compute $\Delta c_{A_{1g}}$, we solve the 2D Hubbard model with the cellular extension²⁶⁻²⁸ of dynamical mean-field theory⁵. We solve the cluster -here a 2×2 plaquette- quantum impurity problem using a continuous time quantum Monte Carlo method^{29,30} in the hybridisation expansion of the impurity action. We focus on the normal state only.

III. PHASE DIAGRAM

To understand the features of the velocity of sound of the 2D compressible Hubbard model, we briefly review

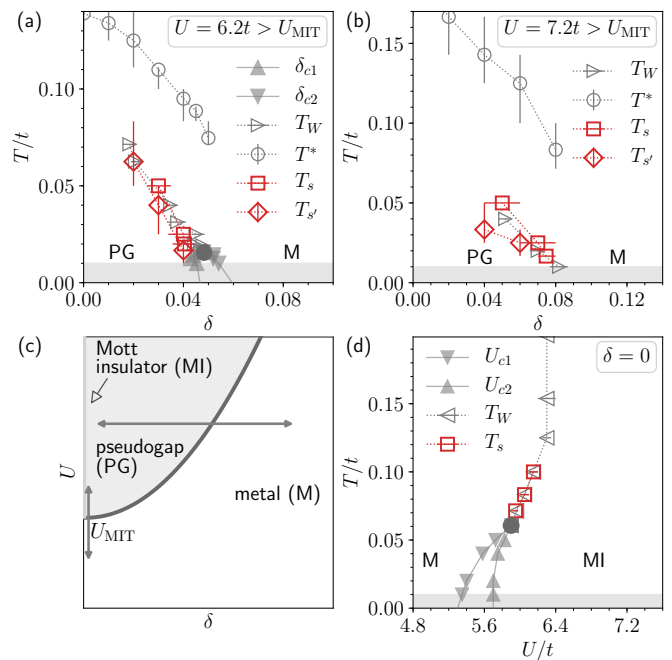


FIG. 1. (a,b) Temperature versus doping normal state phase diagram, as obtained from the CDMFT solution of the 2D Hubbard model (gray symbols). Data are obtained for $U = 6.2t$ and $U = 7.2t$, which set the system in the doped Mott insulator regime. At finite doping there is a first-order phase transition between a pseudogap (PG) and a metal (M). This transition is bounded by the spinodals δ_{c1} and δ_{c2} (filled triangles) and ends at a critical endpoint (filled dark gray circle). From the endpoint emerges the Widom line, T_W , here defined as the loci of the peaks in the isothermal charge compressibility κ as a function of doping for different temperatures. The open circles denote where the spin susceptibility drops versus T at fixed doping, signalling the onset temperature of the pseudogap T^* . (c) Sketch of the interaction strength U versus doping normal state phase diagram of the 2D Hubbard model. (d) Temperature versus U normal state phase diagram for the half filled model ($\delta = 0$). The first-order metal to Mott insulator transition is bounded by spinodals U_{c1} and U_{c2} (filled triangles), ending in a critical endpoint (filled circle), from which emanates the Widom line, a supercritical crossover (open triangles) defined by the loci of the inflection in the double occupancy versus U at fixed T . Gray symbols are taken from Refs.^{31,36}. Red symbols are the new results of this work and indicate the loci of the minima in the velocity of sound versus δ at fixed T (squares in panels a, b) or versus U at fixed T (squares in panel d), or versus δ (diamonds in panels a, b). These minima are one of the main findings of this article. Shaded area at low T in panels a, b, d corresponds to the region that is inaccessible because of the fermionic sign problem.

the main aspects of the phase diagram of the underlying 2D Hubbard model. Hole-doped cuprates are doped Mott insulators. To set the system in this regime, we use a value of the interaction larger than threshold U_{MIT} necessary to open a Mott gap at zero doping. Figure 1a

shows the normal state temperature - doping phase diagram for $U = 6.2t$ emerging from the CDMFT solution of the 2D Hubbard model³¹. At low temperature there is a first-order transition at finite doping and finite temperature between a strongly correlated metal with a pseudogap and a correlated metal. This normal state transition is actually hidden beneath a superconducting dome^{6,32,34}. It is first-order and ends in a second-order critical endpoint (gray filled circle). From the endpoint emerge some crossover lines in the thermodynamic^{8,9,35} and entanglement³⁶ properties with the features of the Widom line T_W . The crossover line defining the onset temperature of the pseudogap T^* ends abruptly at δ_p ^{9,11}, as found in experiments^{37,38}, and is a high-temperature precursor of T_W . The pseudogap to metal transition is a purely electronic metal to metal transition, and the two phases have the same symmetries.

To reveal the origin of this pseudogap to metal transition without symmetry breaking, it is necessary to vary the interaction U . Figure 1b shows the $T - \delta$ phase diagram for $U = 7.2t$. Upon increasing U , the pseudogap to metal transition moves to larger doping and lower temperature. The Widom line can be used to reveal the existence of the pseudogap to metal transition, which in Figure 1b occurs at a low temperature currently inaccessible due to the fermionic sign problem⁷. By further varying the interaction U , one obtains^{6,7} the schematic $U - \delta$ normal-state phase diagram sketched in Figure 1c. By following the horizontal arrow in the doped Mott insulator regime, the system evolves from a Mott insulator at zero doping to a pseudogap followed by a first-order transition to a metal. The pseudogap to metal transition (thick gray line) is connected to the metal to Mott insulator transition at zero doping (vertical arrow and the resulting $U - T$ phase diagram in Figure 1d). This implies^{6,7} that the pseudogap to metal transition originates from Mott physics and short-range correlations. Physically, this means Mott localisation plus short range correlations, arising from superexchange, form singlet bonds that open a pseudogap.

The crossing of the Widom line and its underlying second order critical line ending the first-order transition gives rise to a peak in the electronic specific heat¹⁰. This provides a microscopic framework that solves the apparent paradox raised by recent experiments² reporting a sharp peak in the low temperature normal state electronic specific heat at the doping δ_p where the pseudogap ends without evidence of broken symmetry states. Our main contribution here is to show that thermodynamic anomalies –such as the peak along the Widom line in the electronic specific heat and in the charge compressibility– are also imprinted in the velocity of sound. We shall show that the isothermal velocity of sound for the A_{1g} mode has anomalies in the form of sharp dips versus δ upon crossing the endpoint of the pseudogap to metal transition and its associated Widom line. Red squares in Figure 1a,b mark the doping levels of the dip in the velocity of sound.

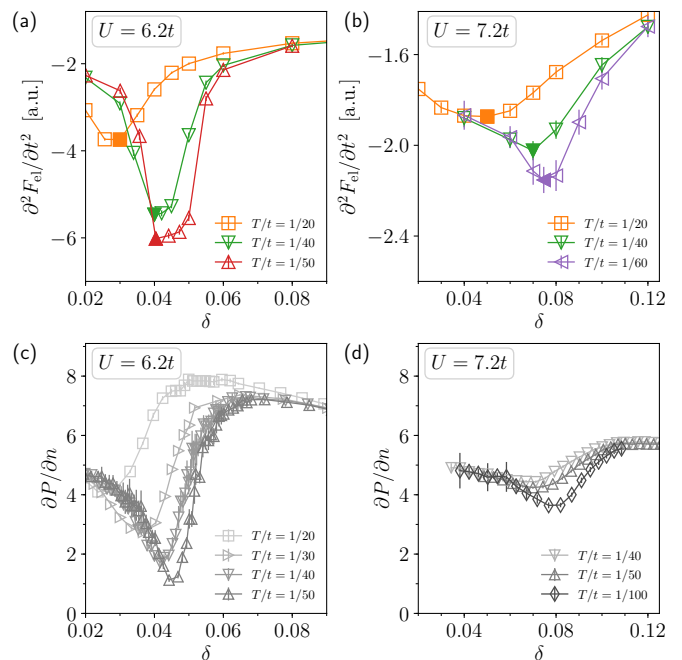


FIG. 2. Upper panels: correction $\Delta c_{A_{1g}}$ to the elastic constant $c_{A_{1g}}$ due to the electron-lattice interaction, as a function of doping and for different temperatures. This elastic constant determines the velocity of sound of the A_{1g} mode. Refer to the supplemental material for the proportionality constants. Minima at finite doping are visible (filled symbols). The loci of the minima vs δ of the velocity of sound are shown by red squares (T_s) in Fig. 1a,b. Lower panels: velocity of sound of the electron gas $v_s^2 \propto \partial P/\partial n$, as a function of doping and for different temperatures. Gray colors emphasise this quantity is at zero strain. Data are shown for $U = 6.2t$ (panels a, c) and $U = 7.2t$ (panels b, d). Error bars indicate the rms error.

IV. VELOCITY OF SOUND IN A DOPED MOTT INSULATOR

Figure 2a,b shows $\partial^2 F_{el}/\partial t^2$ for the correction $\Delta c_{A_{1g}}$ to the elastic constant $c_{A_{1g}}$ due to the electron-lattice interaction, as a function of doping for different temperatures. This term is proportional to the correction to the velocity of sound for the A_{1g} mode, and has also been calculated in Ref.⁵ in the half-filled case.

The velocity of sound has an anomaly, in the form of a dip with a minimum (indicated by the filled symbols), as a function of doping. The dip becomes more pronounced with decreasing temperature. To understand the origin of this dip, we track the doping levels at which the dips occur for different temperatures. This result is shown in Figure 1a,b on the temperature-doping phase diagram, with red squares. The positions of the dips define a crossover line (open red squares in Figure 1a,b) emerging from the critical endpoint of the pseudogap-metal transition. Therefore, the anomaly in the velocity of sound for the A_{1g} mode is a signature of the critical point at finite doping and finite temperature and of its

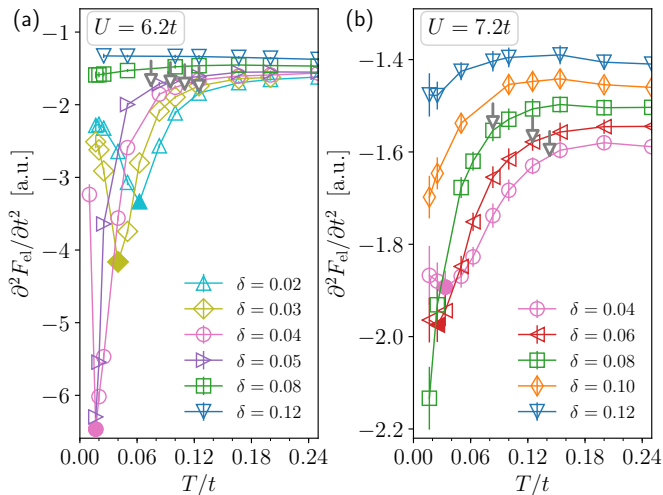


FIG. 3. Correction $\Delta c_{A_{1g}}$ to the elastic constant $c_{A_{1g}}$ due to the electron-lattice interaction, as a function of temperature for different values of doping. This quantity is proportional to the velocity of sound of the A_{1g} mode. Data are obtained for $U = 6.2t$ (a) and $U = 7.2t$ (b). The gray arrows indicate the temperature T^* at each doping level for the underlying 2D Hubbard model (gray open circles in Fig. 1a,b). The curves show a dip (filled symbols) upon crossing the Widom line. The loci of the dips vs T of the velocity of sound are shown by red diamonds ($T_{s'}$) in Fig. 1a,b. Error bars indicate the rms error.

associated crossover in the supercritical region.

To further connect the anomaly in the velocity of sound with earlier results on compressibility anomaly⁸, we calculate the velocity of sound of the electron gas at zero strain estimated from the density-density correlation function at zero strain. Namely, we calculate $v_s^2 \propto (\partial P / \partial n)_T$, where P is the electronic pressure at zero strain, which is associated with the electronic compressibility $\kappa = 1/n^2(\partial n / \partial \mu)$ via $\partial P / \partial n = 1/(n\kappa)$ ^{31,36}. Figure 2c,d shows the velocity of sound of the electron gas as a function of doping for different temperatures. The curves show a dip that becomes more pronounced as the endpoint is approached. The presence of this minimum in the velocity of sound of the electron gas v_s suggests an electronic origin of the anomaly in the velocity of sound c_s for the A_{1g} mode.

Next, let us discuss the onset temperature of the pseudogap, T^* , which is a precursory crossover of this metal to metal transition. Because of this, the velocity of sound should be continuous across T^* . This expectation is fully confirmed by our calculations. Figure 3a,b shows the velocity of sound of the A_{1g} mode as a function of temperature, for different values of doping. The vertical gray arrows indicate the temperature T^* at each doping level for the underlying 2D Hubbard model (see Figure 1a,b). Within our numerical uncertainty, the velocity of sound is continuous and does not show any particular features across T^* . Note that the velocity of sound shows a min-

imum versus T (filled symbols in Figure 3a,b and red diamonds in Figure 1a,b) upon crossing T_W . The low temperature hardening signals the electrons locking into singlets due to superexchange.

V. VELOCITY OF SOUND AT HALF FILLING

Since the pseudogap to metal transition is connected to the metal to Mott insulator transition in the interaction-doping plane (Figure 1c), we shall discuss the behavior of the velocity of sound at half filling, across the metal to Mott insulator transition.

The velocity of sound of the A_{1g} mode has a minimum as a function of U/t (see Supplemental Material²⁵). Most importantly, this minimum defines a crossover line in the supercritical region (red squares in Figure 1d), which lies close to the Widom line (gray open triangles in Figure 1d). This dip is a signature of the Mott critical point and its associated crossover. This result for the sound velocity versus U at half filling confirms and extends the findings of Hassan et al.⁵ for the 3D compressible Hubbard model solved with single-site DMFT.

VI. DISCUSSION

Using the 2D compressible Hubbard model, we have calculated the isothermal velocity of sound for the A_{1g} mode with CDMFT, and shown it has a sharp dip versus doping. At low temperature, this anomaly signals a second order critical endpoint at finite temperature and finite doping, which is the endpoint of the pseudogap to metal transition. This is a purely electronic transition without symmetry breaking. Upon increasing T away from the endpoint, the dip becomes shallower and its locus delineates a supercritical crossover line emanating from the endpoint (red squares in Figure 1a,b).

We predict that ultrasound experiments in hole doped cuprates should observe a minimum in the velocity of sound for the A_{1g} mode at the doping δ_p where the pseudogap ends, once superconductivity is removed by a magnetic field. Furthermore, this dip should become sharper with decreasing temperature. These predicted anomalies indicate the existence of an electronic transition without symmetry breaking, from which supercritical crossovers emerge. This transition is hidden by the superconducting phase^{6,32,34,39}. Verifying this prediction in experiments would be a worthy challenge to explore as it may help to unlock the elusive nature of the pseudogap phase.

This dip parallels the peak at δ_p in the electronic specific heat recently observed in the LSCO family^{2,40} and successfully modeled by the 2D Hubbard model¹⁰. Given that both specific heat and velocity of sound are thermodynamic indicators of the system, our results provide additional thermodynamic constraints and show that the minimum in the velocity of sound versus δ is a likely feature of real materials.

Our prediction for hole doped cuprates is strengthened by the following observation. The pseudogap to metal transition is connected in the $U - \delta - T$ space to the Mott transition at zero doping (Figure 1c) where a minimum in the velocity of sound has already been detected in V_2O_3 ¹⁹ and in the organic superconductors^{5,20}, with a relative decrease of 2% and 20% respectively.

While the low temperature crossing of δ_p reveals a minimum in the velocity of sound of the A_{1g} mode versus doping, our calculation shows no signs of a phase transition occurring versus temperature across the onset temperature T^* . Ultrasound measurements^{12,14} find an overall hardening of the sound velocity as temperature decreases, as expected from background anharmonic-phonon effects. Since we are interested in how conduction

electrons influence the sound velocity, that background must be subtracted. We hope that our results may guide further experimental investigations.

ACKNOWLEDGMENTS

We are indebted to Claude Bourbonnais, Cyril Proust, and Antoine Georges for useful discussions. This work has been supported by the Canada First Research Excellence Fund. Simulations were performed on computers provided by the Canadian Foundation for Innovation, the Ministère de l'Éducation des Loisirs et du Sport (Québec), Calcul Québec, and Compute Canada.

* corresponding author: giovanni.sordi@rhul.ac.uk

- ¹ Cyril Proust and Louis Taillefer, “The remarkable underlying ground states of cuprate superconductors,” *Annual Review of Condensed Matter Physics* **10**, 409–429 (2019).
- ² B. Michon, C. Girod, S. Badoux, J. Kačmarčík, Q. Ma, M. Dragomir, H. A. Dabkowska, B. D. Gaulin, J. S. Zhou, S. Pyon, T. Takayama, H. Takagi, S. Verret, N. Doiron-Leyraud, C. Marcenat, L. Taillefer, and T. Klein, “Thermodynamic signatures of quantum criticality in cuprates,” *Nature* **567**, 218–222 (2019).
- ³ B. Keimer, S. A. Kivelson, M. R. Norman, S. Uchida, and J. Zaanen, “From quantum matter to high-temperature superconductivity in copper oxides,” *Nature* **518**, 179–186 (2015).
- ⁴ Henri Alloul, “What is the simplest model that captures the basic experimental facts of the physics of underdoped cuprates?” *Comptes Rendus Physique* **15**, 519 – 524 (2014).
- ⁵ Antoine Georges, Gabriel Kotliar, Werner Krauth, and Marcelo J. Rozenberg, “Dynamical mean-field theory of strongly correlated fermion systems and the limit of infinite dimensions,” *Rev. Mod. Phys.* **68**, 13 (1996).
- ⁶ G. Sordi, K. Haule, and A.-M. S. Tremblay, “Finite Doping Signatures of the Mott Transition in the Two-Dimensional Hubbard Model,” *Phys. Rev. Lett.* **104**, 226402 (2010).
- ⁷ G. Sordi, K. Haule, and A.-M. S. Tremblay, “Mott physics and first-order transition between two metals in the normal-state phase diagram of the two-dimensional Hubbard model,” *Phys. Rev. B* **84**, 075161 (2011).
- ⁸ G. Sordi, P. Sémon, K. Haule, and A.-M. S. Tremblay, “Pseudogap temperature as a Widom line in doped Mott insulators,” *Sci. Rep.* **2**, 547 (2012).
- ⁹ G. Sordi, P. Sémon, K. Haule, and A.-M. S. Tremblay, “c-axis resistivity, pseudogap, superconductivity, and Widom line in doped Mott insulators,” *Phys. Rev. B* **87**, 041101 (2013).
- ¹⁰ G. Sordi, C. Walsh, P. Sémon, and A.-M. S. Tremblay, “Specific heat maximum as a signature of mott physics in the two-dimensional hubbard model,” *Phys. Rev. B* **100**, 121105 (2019).
- ¹¹ A. Reymbaut, S. Bergeron, R. Garioud, M. Thénault, M. Charlebois, P. Sémon, and A.-M. S. Tremblay, “Pseudogap, van hove singularity, maximum in entropy, and specific heat for hole-doped mott insulators,” *Phys. Rev. Research* **1**, 023015 (2019).
- ¹² Arkady Shekhter, B. J. Ramshaw, Ruixing Liang, W. N. Hardy, D. A. Bonn, Fedor F. Balakirev, Ross D. McDonald, Jon B. Betts, Scott C. Riggs, and Albert Migliori, “Bounding the pseudogap with a line of phase transitions in $YBa_2Cu_3O_{6+\delta}$,” *Nature* **498**, 75–77 (2013).
- ¹³ J. R. Cooper, J. W. Loram, I. Kokanović, J. G. Storey, and J. L. Tallon, “Pseudogap in $YBa_2Cu_3O_{6+\delta}$ is not bounded by a line of phase transitions: Thermodynamic evidence,” *Phys. Rev. B* **89**, 201104 (2014).
- ¹⁴ Mehdi Frachet, Igor Vinograd, Rui Zhou, Siham Benhabib, Shangfei Wu, Hadrien Mayaffre, Steffen Krämer, Sanath K. Ramakrishna, Arneil P. Reyes, Jérôme Debray, Tohru Kurosawa, Naoki Momono, Migaku Oda, Seiki Komiya, Shimpei Ono, Masafumi Horio, Johan Chang, Cyril Proust, David LeBoeuf, and Marc-Henri Julien, “Hidden magnetism at the pseudogap critical point of a cuprate superconductor,” *Nature Physics* **16**, 1064–1068 (2020).
- ¹⁵ M. Frachet, S. Benhabib, I. Vinograd, S.-F. Wu, B. Vignolle, H. Mayaffre, S. Krämer, T. Kurosawa, N. Momono, M. Oda, J. Chang, C. Proust, M.-H. Julien, and D. LeBoeuf, “High magnetic field ultrasound study of spin freezing in $La_{1.88}Sr_{0.12}CuO_4$,” *Phys. Rev. B* **103**, 115133 (2021).
- ¹⁶ Sayak Ghosh, Michael Matty, Ryan Baumbach, Eric D. Bauer, K. A. Modic, Arkady Shekhter, J. A. Mydosh, Eun-Ah Kim, and B. J. Ramshaw, “One-component order parameter in URu_2Si_2 uncovered by resonant ultrasound spectroscopy and machine learning,” *Science Advances* **6**, eaaz4074 (2020).
- ¹⁷ S. Benhabib, C. Lupien, I. Paul, L. Berges, M. Dion, M. Nardone, A. Zitouni, Z. Q. Mao, Y. Maeno, A. Georges, L. Taillefer, and C. Proust, “Ultrasound evidence for a two-component superconducting order parameter in Sr_2RuO_4 ,” *Nature Physics* **17**, 194–198 (2020).
- ¹⁸ Sayak Ghosh, Arkady Shekhter, F. Jerzembeck, N. Kikugawa, Dmitry A. Sokolov, Manuel Brando, A. P. Mackenzie, Clifford W. Hicks, and B. J. Ramshaw, “Thermodynamic evidence for a two-component superconducting order parameter in Sr_2RuO_4 ,” *Nature Physics* **17**, 199–204 (2020).
- ¹⁹ S. Populoh, P. Wzietek, R. Gohier, and P. Metcalf, “Lattice softening effects at the Mott critical point of Cr-doped V_2O_3 ,” *Phys. Rev. B* **84**, 075158 (2011).

- ²⁰ D. Fournier, M. Poirier, M. Castonguay, and K. D. Truong, “Mott Transition, Compressibility Divergence, and the P – T Phase Diagram of Layered Organic Superconductors: An Ultrasonic Investigation,” *Phys. Rev. Lett.* **90**, 127002 (2003).
- ²¹ Mario Poirier, Maxime Dion, and David Fournier, “Symmetry-imposed signatures at the pseudogap crossover in κ -(BEDT-TTF) $_2X$ organic superconductors,” *Phys. Rev. B* **83**, 132507 (2011).
- ³ W. P. Su, J. R. Schrieffer, and A. J. Heeger, “Solitons in polyacetylene,” *Phys. Rev. Lett.* **42**, 1698–1701 (1979).
- ⁴ Pinaki Majumdar and H. R. Krishnamurthy, “Lattice Contraction Driven Insulator-Metal Transition in the $d = \infty$ Local Approximation,” *Phys. Rev. Lett.* **73**, 1525–1528 (1994).
- ⁵ S. R. Hassan, A. Georges, and H. R. Krishnamurthy, “Sound Velocity Anomaly at the Mott Transition: Application to Organic Conductors and V_2O_3 ,” *Phys. Rev. Lett.* **94**, 036402 (2005).
- ²⁵ See Supplemental Material for the derivation of the correction to the velocity of sound c_s and for additional results of c_s at half filling.
- ²⁶ Thomas Maier, Mark Jarrell, Thomas Pruschke, and Matthias H. Hettler, “Quantum cluster theories,” *Rev. Mod. Phys.* **77**, 1027–1080 (2005).
- ²⁷ G. Kotliar, S. Y. Savrasov, K. Haule, V. S. Oudovenko, O. Parcollet, and C. A. Marianetti, “Electronic structure calculations with dynamical mean-field theory,” *Rev. Mod. Phys.* **78**, 865 (2006).
- ²⁸ A.-M. S. Tremblay, B. Kyung, and D. Sénéchal, “Pseudogap and high-temperature superconductivity from weak to strong coupling. Towards a quantitative theory,” *Low Temp. Phys.* **32**, 424 (2006).
- ²⁹ Emanuel Gull, Andrew J. Millis, Alexander I. Lichtenstein, Alexey N. Rubtsov, Matthias Troyer, and Philipp Werner, “Continuous-time Monte Carlo methods for quantum impurity models,” *Rev. Mod. Phys.* **83**, 349–404 (2011).
- ³⁰ P. Sémon, Chuck-Hou Yee, Kristjan Haule, and A.-M. S. Tremblay, “Lazy skip-lists: An algorithm for fast hybridization-expansion quantum Monte Carlo,” *Phys. Rev. B* **90**, 075149 (2014).
- ³¹ C. Walsh, P. Sémon, D. Poulin, G. Sordi, and A.-M. S. Tremblay, “Thermodynamic and information-theoretic description of the Mott transition in the two-dimensional Hubbard model,” *Phys. Rev. B* **99**, 075122 (2019).
- ³² G. Sordi, P. Sémon, K. Haule, and A.-M. S. Tremblay, “Strong Coupling Superconductivity, Pseudogap, and Mott Transition,” *Phys. Rev. Lett.* **108**, 216401 (2012).
- ⁶ L. Fratino, P. Sémon, G. Sordi, and A.-M. S. Tremblay, “An organizing principle for two-dimensional strongly correlated superconductivity,” *Sci. Rep.* **6**, 22715 (2016).
- ³⁴ Caitlin Walsh, Maxime Charlebois, Patrick Sémon, Giovanni Sordi, and André-Marie S. Tremblay, “Information-theoretic measures of superconductivity in a two-dimensional doped mott insulator,” *Proceedings of the National Academy of Sciences* **118**, e21041114118 (2021).
- ³⁵ C. Walsh, P. Sémon, G. Sordi, and A.-M. S. Tremblay, “Critical opalescence across the doping-driven mott transition in optical lattices of ultracold atoms,” *Phys. Rev. B* **99**, 165151 (2019).
- ³⁶ C. Walsh, P. Sémon, D. Poulin, G. Sordi, and A.-M. S. Tremblay, “Entanglement and classical correlations at the doping-driven mott transition in the two-dimensional hubbard model,” *PRX Quantum* **1**, 020310 (2020).
- ³⁷ C. Collignon, S. Badoux, S. A. A. Afshar, B. Michon, F. Laliberté, O. Cyr-Choinière, J.-S. Zhou, S. Licciardello, S. Wiedmann, N. Doiron-Leyraud, and Louis Taillefer, “Fermi-surface transformation across the pseudogap critical point of the cuprate superconductor $\text{La}_{1.6-x}\text{Nd}_{0.4}\text{Sr}_x\text{CuO}_4$,” *Phys. Rev. B* **95**, 224517 (2017).
- ³⁸ O. Cyr-Choinière, R. Daou, F. Laliberté, C. Collignon, S. Badoux, D. LeBoeuf, J. Chang, B. J. Ramshaw, D. A. Bonn, W. N. Hardy, R. Liang, J.-Q. Yan, J.-G. Cheng, J.-S. Zhou, J. B. Goodenough, S. Pyon, T. Takayama, H. Takagi, N. Doiron-Leyraud, and Louis Taillefer, “Pseudogap temperature T^* of cuprate superconductors from the nernst effect,” *Phys. Rev. B* **97**, 064502 (2018).
- ³⁹ L. Fratino, P. Sémon, G. Sordi, and A.-M. S. Tremblay, “Pseudogap and superconductivity in two-dimensional doped charge-transfer insulators,” *Phys. Rev. B* **93**, 245147 (2016).
- ⁴⁰ C. Girod, D. LeBoeuf, A. Demuer, G. Seyfarth, S. Imajo, K. Kindo, Y. Kohama, M. Lizaire, A. Legros, A. Gourgout, H. Takagi, T. Kurosawa, M. Oda, N. Momono, J. Chang, S. Ono, G.-q. Zheng, C. Marcnat, L. Taillefer, and T. Klein, “Normal state specific heat in the cuprate superconductors $\text{La}_{2-x}\text{Sr}_x\text{CuO}_4$ and $\text{Bi}_{2+y}\text{Sr}_{2-x-y}\text{La}_x\text{CuO}_{6+\delta}$ near the critical point of the pseudogap phase,” *Phys. Rev. B* **103**, 214506 (2021).

Supplemental Material:
Prediction of anomalies in the velocity of sound for the pseudogap of hole-doped cuprates

C. Walsh, M. Charlebois, P. Sémon, G. Sordi, A.-M. S. Tremblay

In Section I we derive the result for the correction to the velocity of sound c_s of the A_{1g} mode used in the main text. In Section II we provide additional data for the velocity of sound at half filling.

I. DERIVATION OF THE CORRECTION TO THE VELOCITY OF SOUND

A. Definitions

The velocity of sound c_s along high symmetry directions is $c_s = \sqrt{c_{ij}/\rho}$, where ρ is the density and c_{ij} is the elastic constant in the Voigt notation¹. Note that c_{ij} has the units of pressure and is defined as the second derivative of the free energy F with respect to the strain u_{ij} , $c_{ij} = \partial^2 F / \partial u_{ij}^2$, with

$$u_{ij} = \frac{1}{2} \left(\frac{\partial u_i}{\partial r_j} + \frac{\partial u_j}{\partial r_i} \right), \quad (1)$$

where $u_i(\mathbf{r})$ is the displacement along the direction r_i , with $(r_1, r_2, r_3) = (x, y, z)$. Note that the strain u_{ij} is dimensionless, and thus F_{latt} has the units of c_{ij} , i.e. it is a free energy density.

We want to capture the physics of the cuprates, which have tetragonal crystal structure. Hence we consider the point group D_{4h} . The resulting lattice free energy F_{latt} is²

$$F_{\text{latt}} = \frac{1}{2} c_{11} (u_{xx}^2 + u_{yy}^2) + c_{12} u_{xx} u_{yy} + 2c_{66} u_{xy}^2 + \frac{1}{2} c_{33} u_{zz}^2 + c_{13} (u_{xx} + u_{yy}) u_{zz}, \quad (2)$$

with standard Voigt notation for the elastic constants. Furthermore, cuprates are layered materials of 2D planes stacked along the z axis. We shall calculate the longitudinal velocity of sound within the xy plane. Hence we consider only the strain in the xy plane, and neglect the strain in the z direction. Hence we are left to consider the lattice free energy

$$F_{\text{latt}} = \frac{1}{2} c_{11} (u_{xx}^2 + u_{yy}^2) + c_{12} u_{xx} u_{yy}. \quad (3)$$

Furthermore, we shall consider only uniform compressive strain. Hence, it is useful to write F_{latt} using the irreducible representations A_{1g} and B_{1g} of the D_{4h} group. The uniform compression is associated with the A_{1g} mode. The A_{1g} and B_{1g} components of the strain can be written as

$$u_{A_{1g}} = u_{xx} + u_{yy} \quad (4)$$

$$u_{B_{1g}} = u_{xx} - u_{yy}. \quad (5)$$

Hence Eq. 3 becomes:

$$F_{\text{latt}} = \frac{1}{2} \left(c_{A_{1g}} u_{A_{1g}}^2 + c_{B_{1g}} u_{B_{1g}}^2 \right), \quad (6)$$

where the elastic constants for the A_{1g} and B_{1g} modes are

$$c_{A_{1g}} = \frac{1}{2} (c_{11} + c_{12}) \quad (7)$$

$$c_{B_{1g}} = \frac{1}{2} (c_{11} - c_{12}). \quad (8)$$

Therefore the longitudinal velocity of sound that we shall calculate is

$$c_s = \sqrt{\frac{c_{A_{1g}}}{\rho}}. \quad (9)$$

Up until now we have only considered lattice degrees of freedom. We want to describe both lattice and electronic degrees of freedom, i.e. we want to consider

$$F = F_{\text{latt}} + F_{\text{el}} \quad (10)$$

with

$$F_{\text{el}} = F_0 + F_{\text{el-latt}}, \quad (11)$$

where F_0 is the free energy of the electrons at zero strain. As a result, the velocity of sound c_s is renormalised by the interaction with the electrons. Hence we can write:

$$c_s = \sqrt{\frac{c_{A_{1g}}^*}{\rho}}, \quad (12)$$

where

$$c_{A_{1g}}^* = c_{A_{1g}} + \Delta c_{A_{1g}}. \quad (13)$$

The correction $\Delta c_{A_{1g}}$ is coming from the interaction with the electrons. Our goal is thus to find an estimate for $\Delta c_{A_{1g}}$.

B. 2D compressible Hubbard model

To find $\Delta c_{A_{1g}}$, we consider the Su-Schrieffer-Heeger (SSH) Hubbard model³ on a 2D square lattice. To simplify the derivation, we first consider a strain applied in only one direction. Since we consider only nearest neighbor hopping, x and y directions are independent. Potential energy is unaffected, so we need only consider how strain modifies the kinetic energy in the direction of the lattice vector where it is applied, hence we have

$$- \sum_{\langle ij \rangle \sigma} t[a + (d_i - d_j)](c_{i\sigma}^\dagger c_{j\sigma} + c_{j\sigma}^\dagger c_{i\sigma}), \quad (14)$$

where i and j now refer to lattice positions, not cartesian directions as before. We take d_i as the displacement from equilibrium of the atom at position i . This model can be also referred to as a *compressible* Hubbard model, as in Refs.^{4,5}. Here $c_{i\sigma}^\dagger$ and $c_{i\sigma}$ operators create and destroy an electron at site i of spin σ . The equilibrium distance between atoms is a . Contrary to the standard Hubbard model, the nearest neighbor hopping amplitude t in Eq. 14 is not constant, but is modulated by the local change $(d_i - d_j)$ of the equilibrium lattice constant a .

A Taylor expansion of the hopping amplitude t about $(d_i - d_j) = 0$ gives:

$$t[a + (d_i - d_j)] \approx t_{ij} + \frac{\partial t}{\partial a}(d_i - d_j), \quad (15)$$

where the equilibrium value $t(a)$ is denoted by t_{ij} , which is equal to t for nearest neighbor hopping and to zero otherwise. Therefore the hopping term K_{el} that is modified by $d_i - d_j$ can be written as:

$$K_{\text{el}} = K_0 + K_{\text{el-latt}} \quad (16)$$

$$= - \sum_{\langle ij \rangle \sigma} t_{ij}(c_{i\sigma}^\dagger c_{j\sigma} + c_{j\sigma}^\dagger c_{i\sigma}) - \sum_{\langle ij \rangle \sigma} \frac{\partial t}{\partial a}(d_i - d_j)(c_{i\sigma}^\dagger c_{j\sigma} + c_{j\sigma}^\dagger c_{i\sigma}), \quad (17)$$

where K_0 is the familiar hopping term in the standard Hubbard model at zero strain and $K_{\text{el-latt}}$ is the modulated hopping term as in a SSH-like model.

It is convenient to take the origin of each bond in the middle of two sites. Along the x direction then, we rewrite the change in local interatomic distance in terms of the strain, using the notation of the previous subsection in the long wave-length limit

$$d_i - d_{i+1} = - \left. \frac{\partial u_x(\mathbf{r})}{\partial x} \right|_{\mathbf{r}_k} a, \quad (18)$$

where $\mathbf{r}_k = (\mathbf{r}_{i+1} - \mathbf{r}_i)/2$, and where index k labels bonds. We rewrite the second-quantized operators in this basis and define $\epsilon_x(\mathbf{r}_k)$ as follows

$$c_i^\dagger c_{i+1} = c_{\mathbf{r}_k - a/2}^\dagger c_{\mathbf{r}_k + a/2} = \epsilon_x(\mathbf{r}_k). \quad (19)$$

because stretched bonds are in the x direction.

Then the electron-lattice interaction $K_{\text{el-latt}}$ in Eq. 17 along the x direction becomes

$$\sum_{x_k} \left(-a \frac{\partial t}{\partial a} \right) u_{xx}(\mathbf{r}_k) \left(c_{\mathbf{r}_k - a/2}^\dagger c_{\mathbf{r}_k + a/2} + h.c. \right) = g \sum_{x_k} u_{xx}(\mathbf{r}_k) (\epsilon_x(\mathbf{r}_k) + h.c.), \quad (20)$$

with the definition

$$g = -a \frac{\partial t}{\partial a}. \quad (21)$$

The result is similar in the y direction. Note that g has units of energy and that $g > 0$ is satisfied because t decreases when a increases.

Next we move to reciprocal space assuming a single wave-vector. And since we consider uniform compressive strain we will eventually take the $q \rightarrow 0$ limit. Taking the Fourier transform of the strain gives:

$$u_{xx}(\mathbf{r}_k) = u_{xx}(\mathbf{q}) (e^{i\mathbf{q}\cdot\mathbf{r}} + e^{-i\mathbf{q}\cdot\mathbf{r}}) / 2, \quad (22)$$

where \mathbf{q} is in the x direction and $q \rightarrow 0$. Then the interaction Eq. 20 becomes (since $u_{xx}(q) = u_{xx}(-q)$):

$$g \frac{u_{xx}(q)}{2} (\epsilon_x^-(q) + \epsilon_x^+(q)) + g \frac{u_{xx}(-q)}{2} (\epsilon_x^-(q) + \epsilon_x^+(q)), \quad (23)$$

with a similar result in the y direction. Here ϵ^+ and ϵ^- denote the two terms entering the kinetic energy. Both $u_{xx}(q)$ and ϵ_x^\pm are dimensionless.

Bringing together the terms along the x and y directions, we obtain:

$$K_{\text{el-latt}} = g [\epsilon_x(-q)u_{xx}(q)/2 + \epsilon_x(q)u_{xx}(-q)/2] + g [\epsilon_y(-q)u_{yy}(q)/2 + \epsilon_y(q)u_{yy}(-q)/2], \quad (24)$$

where we defined:

$$\epsilon_x(q) = \epsilon_x^-(q) + \epsilon_x^+(q) \quad (25)$$

$$\epsilon_y(q) = \epsilon_y^-(q) + \epsilon_y^+(q). \quad (26)$$

Our aim is to trace over the electronic degrees of freedom to find out how F_{latt} is modified. For completeness then, let us also write F_{latt} in reciprocal space. For clarity, let us focus only on u_{xx} with a single wave-vector as above. We find

$$F_{\text{latt}} = \int \frac{1}{2} c_{11} u_{xx}(\mathbf{r}) u_{xx}(\mathbf{r}) d\mathbf{r} = \frac{1}{2} c_{11} \frac{u_{xx}(q)u_{xx}(-q)}{2}. \quad (27)$$

C. Correction to the elastic free energy from coupling to the conduction electrons

We take the following steps, valid only for a Hubbard model with nearest neighbor hopping. Otherwise, the operator for the stress tensor is more complicated. First we find the correction to the elastic free-energy to second-order in g for a simple strain u_{xx} . We obtain a zero-frequency Matsubara response function as the correction, a result identical to what we would have obtained from a phonon self-energy-calculation for this model. Second we trivially extend the result to a A_{1g} strain. Finally, we rewrite the result for the correction to the elastic constant $c_{A_{1g}}$ in terms of a derivative of the kinetic energy.

1. Perturbative result for the free energy

The contribution to the elastic stiffness due to the conduction electrons is obtained by tracing over them. In other words, in this section we are focusing on the contributions to the partition function that comes from the electronic Hamiltonian and from the interaction of the electrons with the lattice. We assume that the elastic free energy without the conduction electrons is already known.

As before, we can separate the strains along the x and y direction. Let us focus on the x direction. We take the strain u_{xx} as a *classical* variable that commutes with the electronic Hamiltonian. We can also now take the $q \rightarrow 0$

limit without worrying because ϵ_x is not conserved, so the $q \rightarrow 0$ limit and the zero-frequency limit can be taken in any order. Therefore, in the interaction representation, the partition function of the electrons including the contributions of the strain is:

$$Z = \text{Tr}_{\text{el}} \left[e^{-\beta H_{\text{el}}} T_{\tau} e^{-\int_0^{\beta} d\tau g[\epsilon_x(0, \tau) u_{xx}(0)]} \right], \quad (28)$$

where T_{τ} is the imaginary-time ordering operator, H_{el} is the electronic Hamiltonian ($-\mu N$) that includes the Hubbard term and the operator $\epsilon_x(0, \tau)$ in imaginary time is given by the usual Heisenberg imaginary-time evolution

$$\epsilon_x(0, \tau) = e^{H_{\text{el}}\tau} \epsilon_x(0) e^{-H_{\text{el}}\tau}. \quad (29)$$

Expanding the exponential to second order, we obtain:

$$Z = Z_0 \left\langle 1 - \int_0^{\beta} d\tau g[\epsilon_x(0, \tau)] u_{xx}(0) + \frac{1}{2} \int_0^{\beta} d\tau \int_0^{\beta} d\tau' g^2 T_{\tau} [\epsilon_x(0, \tau) \epsilon_x(0, \tau')] u_{xx}(0) u_{xx}(0) \right\rangle. \quad (30)$$

Here the brackets refer to a thermal average with the electronic Hamiltonian at zero strain. The partition function at zero strain is denoted Z_0 and the corresponding free energy F_0 . For conciseness, we drop from now on the label that indicates that the variables are evaluated at $q = 0$. Finally then, the contribution to the free energy from the conduction electrons is given by

$$F_{\text{el}} = -\frac{1}{\beta} \ln Z = F_0 - \frac{1}{\beta} \ln [\langle 1 \rangle - g \langle X \rangle + g^2 \langle Y \rangle], \quad (31)$$

where

$$X = \int_0^{\beta} d\tau \epsilon_x(\tau) u_{xx} \quad (32)$$

is first order in u_{xx} and

$$Y = \frac{1}{2} \int_0^{\beta} d\tau \int_0^{\beta} d\tau' T_{\tau} [\epsilon_x(\tau) \epsilon_x(\tau')] u_{xx} u_{xx} \quad (33)$$

is second order in u_{xx} . Expanding the natural logarithm to second order in $g u_{xx}$ we thus obtain:

$$F_{\text{el}} = F_0 - \frac{1}{\beta} \left[g \langle -X \rangle + g^2 \langle Y \rangle - \frac{g^2}{2} \langle X \rangle^2 \right]. \quad (34)$$

The first term in the square brackets is a shift of the zero of the strain. Substituting the above definitions of X and Y in the last equation, we are left with

$$F_{\text{el}} = F_0 - \frac{g^2}{\beta} \left[\int_0^{\beta} d\tau \int_0^{\beta} d\tau' \langle T_{\tau} \epsilon_x(\tau) \epsilon_x(\tau') \rangle - \left[\int_0^{\beta} d\tau \langle \epsilon_x(\tau) \rangle \right]^2 \right] \frac{u_{xx} u_{xx}}{2}. \quad (35)$$

The cyclic property of the trace, equivalently imaginary-time translation invariance, leads to $\langle \epsilon_x(\tau) \rangle = \langle \epsilon_x \rangle$ independent of τ . In the first term, we need to take into account the definition of the time-ordering operator, which leads to

$$\int_0^{\beta} d\tau \int_0^{\beta} d\tau' \langle T_{\tau} \epsilon_x(\tau) \epsilon_x(\tau') \rangle = 2 \int_0^{\beta} d\tau \int_0^{\tau} d\tau' \langle \epsilon_x(\tau) \epsilon_x(\tau') \rangle. \quad (36)$$

Changing variables to

$$\mathcal{T} = (\tau + \tau')/2; \quad \Delta\tau = \tau - \tau' \quad (37)$$

the Jacobian is unity and the integral becomes

$$2 \int_0^{\beta} d\tau \int_{\tau}^{\beta} d\tau' \langle \epsilon_x(\tau') \epsilon_x(\tau) \rangle = 2 \left[\int_0^{\beta/2} d\mathcal{T} \int_0^{l(\mathcal{T})} d\Delta\tau \langle \epsilon_x(\Delta\tau) \epsilon_x(0) \rangle + \int_{\beta/2}^{\beta} d\mathcal{T} \int_0^{u(\mathcal{T})} d\Delta\tau \langle \epsilon_x(\Delta\tau) \epsilon_x(0) \rangle \right] \quad (38)$$

$$= \beta \int_0^{\beta} d\Delta\tau \langle \epsilon_x(\Delta\tau) \epsilon_x(0) \rangle. \quad (39)$$

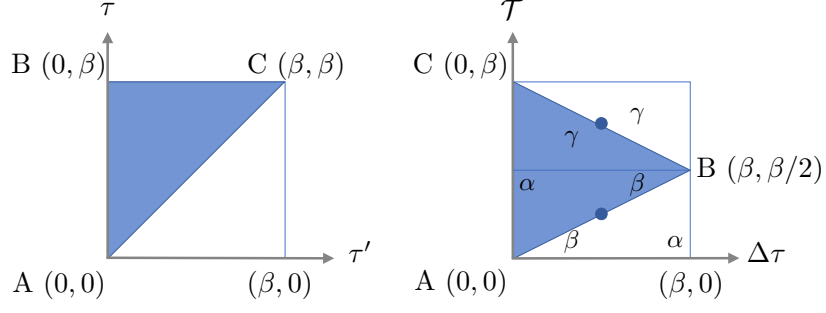


FIG. S1. Change of the integration domain for the time ordered product, on the left, with the change of variables $\mathcal{T} = (\tau + \tau')/2$; $\Delta\tau = \tau - \tau'$ on the right. The (τ, τ') coordinates, abbreviated A, B, C on the left keep the same labels in the $(\Delta\tau, \mathcal{T})$ coordinates on the right. The greek letters indicate examples of points where the function has the same value given that the integrand is independent of \mathcal{T} and that Eq. 40 implies that $\langle \epsilon_x(\Delta\tau - \beta/2)\epsilon_x(0) \rangle = \langle \epsilon_x(\beta/2 - \Delta\tau)\epsilon_x(0) \rangle$. The points on the lower two triangles (blue and transparent) are related by inversion symmetry about $(\Delta\tau/2, \beta/4)$ and those on the upper two triangles by inversion symmetry about $(\Delta\tau/2, 3\beta/4)$. Blue dots mark the latter points.

The last equality can be proven as follows. The domain of integration in the $\mathcal{T}, \Delta\tau$ plane on the right-hand side of the first equality is displayed to the right of Fig. S1. The integral over $\Delta\tau$ for a given \mathcal{T} is over the length of the segment starting at 0 and ending at the lower $l(\mathcal{T})$ or upper $u(\mathcal{T})$ boundaries of the triangle on the right of the figure. However, as we show momentarily, the equality

$$\langle \epsilon_x(\Delta\tau)\epsilon_x(0) \rangle = \langle \epsilon_x(\beta - \Delta\tau)\epsilon_x(0) \rangle \quad (40)$$

holds, so that twice the integral over the triangular region is equal to the integral over the square (see caption of Fig. S1), leading to the desired result Eq. 39 since the integral over $\Delta\tau$, with $\Delta\tau$ always from 0 to β , is independent of \mathcal{T} and the integral over \mathcal{T} gives β . To prove the last equality, Eq. 40, it suffices to use the cyclic property of the trace, as in the equation below, where ψ_x has been used as a proxy for ϵ_x to ease the reading of the proof:

$$\text{Tr} [e^{-\beta H} e^{H\Delta\tau} \epsilon_x e^{-H\Delta\tau} \psi_x] = \text{Tr} [e^{-H\Delta\tau} \psi_x e^{-\beta H} e^{H\Delta\tau} \epsilon_x] \quad (41)$$

$$= \text{Tr} [(e^{-\beta H} e^{\beta H}) e^{-H\Delta\tau} \psi_x e^{-\beta H} e^{H\Delta\tau} \epsilon_x]. \quad (42)$$

Substituting the result of the integral Eq. 39 in our previous expression for the free-energy Eq. 35, the final expression takes the form

$$F_{\text{el}} = F_0 - g^2 \left[\int_0^\beta d\tau \langle \epsilon_x(\tau)\epsilon_x(0) \rangle - \beta \langle \epsilon_x \rangle^2 \right] \frac{u_{xx}u_{xx}}{2}. \quad (43)$$

The renormalization of the elastic constant that one can read from this equation is exactly what one would have obtained from the polarization operator for the self-energy of phonons in the nearest neighbor SSH-Hubbard model for $q \rightarrow 0$. The zero-frequency Matsubara frequency appears in the answer, as we expect for thermodynamic quantities. In general this is the quantity we should compute. It is quite complicated to do this calculation rigorously including vertex corrections. We are going to find an expression that is more convenient to obtain numerically and that contains vertex corrections. But first, let us find the expression for a A_{1g} strain.

2. Response to the A_{1g} mode

By applying a uniform strain in both the x and y directions, we can find the response to a A_{1g} mode. First, we invert Eqs. 4, 5 and find

$$u_{xx} = (u_{A_{1g}} + u_{B_{1g}})/2 \quad (44)$$

$$u_{yy} = (u_{A_{1g}} - u_{B_{1g}})/2. \quad (45)$$

Rewriting the coupling of the strain in both directions in terms of irreducible representations, we find

$$u_{xx}\epsilon_x + u_{yy}\epsilon_y = \frac{1}{2}u_{A_{1g}}(\epsilon_x + \epsilon_y) + \frac{1}{2}u_{B_{1g}}(\epsilon_x - \epsilon_y). \quad (46)$$

If we have only $u_{A_{1g}}$, we couple to the total kinetic energy at $q \rightarrow 0$. We can redo the above derivation to compute the correction to the free energy for a A_{1g} mode. The steps are identical. Hence we find

$$F_{\text{el}} = F_0 - \frac{g^2}{4} \left[\int_0^\beta d\tau \langle \epsilon(\tau)\epsilon(0) \rangle - \beta \langle \epsilon \rangle^2 \right] \frac{1}{2}u_{A_{1g}}^2, \quad (47)$$

which is valid only for nearest neighbors, as we have already mentioned, i.e. for

$$\epsilon = \epsilon_x(q=0) + \epsilon_y(q=0) \quad (48)$$

$$= 2 \sum_{k\sigma} (\cos k_x a + \cos k_y a) c_{k\sigma}^\dagger c_{k\sigma}. \quad (49)$$

3. Correction to the velocity of sound from a derivative of the kinetic energy

Finally, we show that $\int_0^\beta d\tau \langle T_\tau \epsilon(\tau)\epsilon(0) \rangle - \beta \langle \epsilon \rangle^2$ in Eq. 47 can be evaluated from a derivative of the expectation value for the kinetic energy of the purely electronic Hamiltonian. The expectation value of ϵ at zero strain is

$$\langle \epsilon \rangle = \frac{\text{Tr}_{\text{el}} [\epsilon e^{-\beta[-t\epsilon+V]}]}{\text{Tr}_{\text{el}} [e^{-\beta[-t\epsilon+V]}]}, \quad (50)$$

where V contains the Hubbard interaction and the chemical potential contribution. This can be computed from

$$\langle \epsilon \rangle = \frac{1}{\beta} \frac{\partial}{\partial t} \ln Z. \quad (51)$$

even if the commutator $[\epsilon, H_{\text{el}}]$ does not vanish, because the power series of the exponential can be differentiated term by term and re-exponentiated at the end using the cyclic property of the trace. If we take a second derivative, the cyclic property cannot be used to rearrange the expansion of the exponential in a useful manner.

The correct way to approach this problem is to consider the variable $t + dt$ so that $-edt$ is now a perturbation that does not commute with H_{el} . We then need to use the interaction representation so that the partition function is given by

$$Z = \text{Tr}_{\text{el}} \left[e^{-\beta H_{\text{el}}} T_\tau e^{\int_0^\beta d\tau \epsilon(\tau) dt} \right]. \quad (52)$$

Already here, it is clear that the structure of the equation is identical to Eq. 28 obtained in terms of u_{xx} , namely $-gu_{xx}$ is here replaced by dt . So we already know the answer.

Nevertheless, let us give an alternate derivation. Under a time-ordered product, derivatives act as derivatives of real numbers. Hence, to first order

$$\frac{1}{\beta} \frac{\partial}{\partial(dt)} \ln Z = \frac{1}{\beta Z} \text{Tr}_{\text{el}} \left[e^{-\beta H_{\text{el}}} T_\tau e^{\int_0^\beta d\tau \epsilon(\tau) dt} \left(\int_0^\beta d\tau \epsilon(\tau) \right) \right]. \quad (53)$$

The above equation evaluated at zero strain, $dt = 0$, leads to

$$\frac{1}{\beta} \frac{\partial}{\partial t} \ln Z = \frac{1}{Z} \text{Tr}_{\text{el}} [e^{-\beta H_{\text{el}}} \epsilon] = \langle \epsilon \rangle, \quad (54)$$

where we have used the cyclic property of the trace, which is here equivalent to invariance under imaginary-time translation. The chain rule tells us that derivatives with respect to dt are identical to derivatives with respect to t .

The second-order term is obtained by expanding $\ln Z$ to second order without forgetting that after the first order derivative, the partition function Z appearing in the denominator must also be expanded. We find

$$\frac{1}{\beta^2} \frac{\partial^2}{\partial(dt)^2} \ln Z = \frac{1}{\beta^2 Z} \text{Tr}_{\text{el}} \left[e^{-\beta H_{\text{el}}} T_\tau e^{\int_0^\beta d\tau \epsilon(\tau) dt} \left(\int_0^\beta d\tau \epsilon(\tau) \right) \left(\int_0^\beta d\tau' \epsilon(\tau') \right) \right] - \langle \epsilon \rangle^2, \quad (55)$$

where the last term comes from the expansion of Z in the denominator of the first-order result. Evaluating at zero strain, $dt = 0$, and using the definition of the time-ordered product along with invariance under imaginary-time translation as we did from Eqs. 36 to 39, we are left with

$$\frac{1}{\beta^2} \frac{\partial^2}{\partial t^2} \ln Z = \frac{1}{\beta} \frac{\partial}{\partial t} \langle \epsilon \rangle = \frac{1}{\beta Z} \text{Tr}_{\text{el}} \left[e^{-\beta H_{\text{el}}} \int_0^\beta \epsilon(\tau) \epsilon(0) d\tau \right] - \langle \epsilon \rangle^2 \quad (56)$$

$$= \frac{1}{\beta} \int_0^\beta d\tau \langle \epsilon(\tau) \epsilon(0) \rangle - \langle \epsilon \rangle^2. \quad (57)$$

Since the free energy $F_{\text{el}} = F_0 + F_{\text{el-latt}}$ is defined by $F_{\text{el}} = \frac{1}{\beta} \ln Z$, we can substitute this last result in our expression for the free energy Eq. 47 to find

$$F_{\text{el}} = F_0 - \frac{g^2}{4} \frac{\partial \langle \epsilon \rangle}{\partial t} \frac{1}{2} u_{A_{1g}}^2. \quad (58)$$

Therefore, the correction $\Delta c_{A_{1g}}$ to the elastic constant $c_{A_{1g}}$ due to the electron-lattice interaction is

$$\Delta c_{A_{1g}} = \frac{\partial^2 F_{\text{el}}}{\partial u_{A_{1g}}^2} \quad (59)$$

$$= -\frac{g^2}{4} \frac{\partial \langle \epsilon \rangle}{\partial t} \Big|_{U, T, \mu}, \quad (60)$$

which, using $F_{\text{el}} = -\ln Z/\beta$ and Eq. 56 may be rewritten as

$$\Delta c_{A_{1g}} = \frac{g^2}{4} \frac{\partial^2 F_{\text{el}}}{\partial t^2}. \quad (61)$$

This has units of energy density as required. In Eq. 60 we have specified explicitly that the partial derivative is at constant U, T, μ .

For the numerical results in the main text, we compute the derivative $\partial \langle \epsilon \rangle / \partial t$ in Eq. 60 using centered differences with respect to t , with a mesh of $\Delta t = 0.005$. To obtain the kinetic energy $t \langle \epsilon \rangle$ we use the method described in Ref.⁶.

II. EXTENDED DATA FOR THE VELOCITY OF SOUND AT HALF FILLING

In this section we present additional data supporting that the estimate for the velocity of sound of the A_{1g} mode shows a minimum versus U/t at half filling. Figure S2 shows the velocity of sound of the A_{1g} mode as a function of U/t at half filling ($\delta = 0$) and for different temperatures. The curves show a minimum versus U/t (filled symbols). The position of the minima are shown as red squares in Figure 1 of the main text.

* corresponding author: giovanni.sordi@rhul.ac.uk

¹ L. D. Landau, L. P. Pitaevskii, E. M. Lifshitz, and A. M. Kosevich, *Theory of Elasticity*, 3rd ed. (Butterworth-Heinemann, Oxford, 1986).

² S. Benhabib, C. Lupien, I. Paul, L. Berges, M. Dion, M. Nardone, A. Zitouni, Z. Q. Mao, Y. Maeno, A. Georges, L. Taillefer, and C. Proust, “Ultrasound evidence for a two-component superconducting order parameter in Sr_2RuO_4 ,” *Nature Physics* **17**, 194–198 (2020).

³ W. P. Su, J. R. Schrieffer, and A. J. Heeger, “Solitons in polyacetylene,” *Phys. Rev. Lett.* **42**, 1698–1701 (1979).

⁴ Pinaki Majumdar and H. R. Krishnamurthy, “Lattice Contraction Driven Insulator-Metal Transition in the $d = \infty$ Local Approximation,” *Phys. Rev. Lett.* **73**, 1525–1528 (1994).

⁵ S. R. Hassan, A. Georges, and H. R. Krishnamurthy, “Sound Velocity Anomaly at the Mott Transition: Application to Organic Conductors and V_2O_3 ,” *Phys. Rev. Lett.* **94**, 036402 (2005).

⁶ L. Fratino, P. Sémon, G. Sordi, and A.-M. S. Tremblay, “An organizing principle for two-dimensional strongly correlated superconductivity,” *Sci. Rep.* **6**, 22715 (2016).

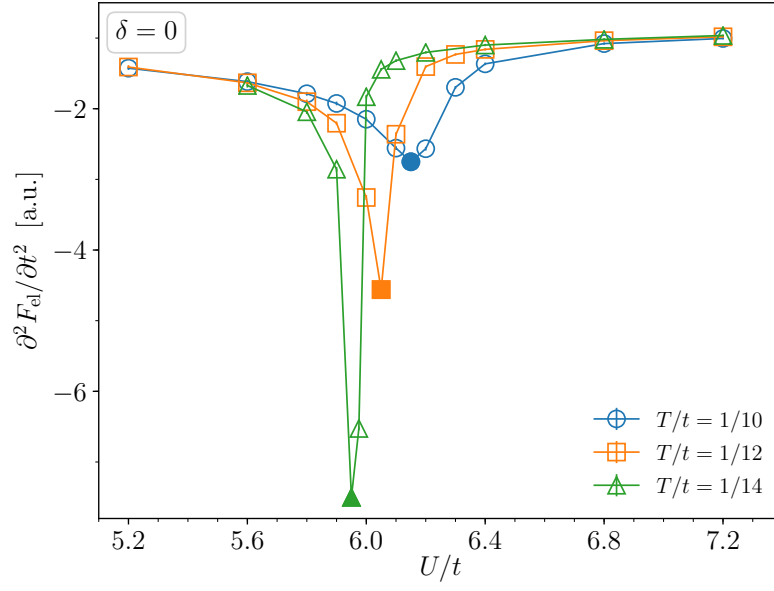


FIG. S2. Correction $\Delta c_{A_{1g}}$ to the elastic constant $c_{A_{1g}}$ due to the electron-lattice interaction, at half filling ($\delta = 0$) as a function of U/t and for different temperatures. A minimum at finite U and finite T is visible (filled symbols). The loci of the minima of the velocity of sound are shown by red squares in the $T - U$ phase diagram of Fig. 1d of the main text.